Eur. Radiol. 9, 1339–1347 (1999)

Pediatric radiology European Radiology

Pictorial review

Pediatric liver neoplasms: a radiologic–pathologic correlation

T. K. Helmberger[1], **P. R. Ros**[2, 3], **P. J. Mergo**[4], **R. Tomczak**[5], **M. F. Reiser**[1]

[1] Institute of Diagnostic Radiology, Klinikum Grosshadern, Ludwig-Maximilians-Universität, Marchioninistrasse 15, D-81366 Munich, Germany
[2] Department of Radiology, Brigham and Women's Hospital, Harvard Medical School, Boston Massachusetts
[3] Department of Radiologic Pathology, Armed Forces Institute of Pathology, Washington, DC, USA
[4] Department of Radiology, University of Florida College of Medicine, Gainesville, Florida, USA
[5] Department of Radiology, University of Ulm, Ulm, Germany

Received: 28 September 1998; Revision received: 22 December 1998; Accepted: 23 December 1998

Abstract. Only 1–2 % of all pediatric tumors occur in the liver. Two thirds of these tumors are malignant and almost all of the tumors cause clinical symptoms due to their mass effects. Besides the poor prognosis in most of the malignant tumors, for further treatment the origin and nature of the neoplasm has to be known. Due to the mostly unimpeded growth into the peritoneal cavity, the origin of the tumors is primarily often unclear and can non-invasively only be determined by advanced imaging techniques. The display of the macro- and microhistological key features of primary pediatric liver neoplasms, including hepatoblastoma (HB), infantile hemangioendothelioma (IHE), mesenchymal hamartoma (MH), undifferentiated (embryonal) sarcoma (UES), and hepatocellular carcinoma (HCC), together with their imaging representation by ultrasound, computed tomography, and magnetic resonance imaging, may deepen the understanding of the underlying pathology and its imaging appearance. Furthermore, in many cases sufficient information may be provided not only to differentiate benign from malignant tumors, but also to guide for adequate treatment.

Key words: Infantile hepatic neoplasm – Radiologic–pathologic correlation – Hepatoblastoma – Embryonal sarcoma – Hemangioendothelioma – Mesenchymal hamartoma

Introduction

Although hepatic neoplasms are relatively infrequent in infants (only 1–2 % of all pediatric tumors occur in the liver), they are clinically relevant since nearly two thirds of them are malignant [1].

The role of imaging in pediatric liver tumors consists of determining first the hepatic origin for an abdominal mass. Once this is accomplished, US, CT, and MRI provide in many cases sufficient information not only to differentiate benign from malignant tumors, but also to guide for an adequate surgical treatment [2].

In this article we present the gamut of primary pediatric liver neoplasms, including hepatoblastoma (HB), infantile hemangioendothelioma (IHE), mesenchymal hamartoma (MH), undifferentiated (embryonal) sarcoma (UES), and hepatocellular carcinoma (HCC; Table 1). Other liver tumors and tumor-like conditions, such as bile duct cysts (or simple cysts), hepatocellular adenoma, and focal nodular hyperplasia, are not discussed due to their extreme rarity in children.

Hepatoblastoma

Hepatoblastoma (synonyms: malignant hepatoblastoma, epithelial and mesenchymal hepatoblastoma, hepatic mixed tumor of childhood) is the most common primary pediatric hepatic tumor accounting for up to 48 % of all malignant pediatric liver tumors. The tumor arises from embryonic and fetal hepatocytes and contains also mesenchymal elements.

The average age at diagnosis is 18 months with a range from birth to 3 years. The male to female ratio is approximately 1.4 to 2:1. The children present with a large palpable abdominal mass, hepatomegaly, abdominal swelling, symptoms of acute abdomen, and fever. Serum alpha-fetoprotein is elevated in up to 90 % of cases, whereas only occasionally there is a positive ß-HCG, producing virilization phenomena, and moderate thrombocytosis. Infrequently, metabolic effects, such as osteopenia with bone fractures, hypercholesterolemia, hypoglycemia, and isosexual precocity, are observed [3, 4]. The general poor prognosis is determined by the tumors extension; however, due to improved chemotherapy regimens survival rates up to 60–70 % are possible [14].

Histologically, HB can be classified into an (a) epithelial, (b) mixed (epithelial/mesenchymal), or (c) ana-

Correspondence to: T. K. Helmberger

Table 1. Clinical findings in pediatric liver tumors. *HB* hepatoblastoma; *IHE* infantile hemangioendothelioma; *MH* mesenchymal hamartoma; *UES* undifferentiated embryonal sarcoma; *HCC* hepatocellular carcinoma

Tumor	Age	Gender (M:F)	Symptoms	Prognosis
HB	18 months (0–3 years)	1.4–2:1	Abdominal mass, hepatomegaly, abdominal swelling, acute abdomen, fever, increased alpha fetoprotein level, hirsutism, thrombocytosis	Poor in extended cases; better if chemotherapy and surgery is applicable
IHE	0–6 months (0–1 year)	1:1.4–2	Abdominal mass, hepatomegaly, congestive heart failure, thrombocytopenia, jaundice, hemoperitoneum (rupture), fetal hydrops	Poor if cardiac decompensation; good if spontaneous involution or resection
MH	15–20 months (0–10 years)	M ≥ F	Painless abdominal mass	Good if resection or decompression
UES	6–12 years	M = F	Abdominal mass, hepatomegaly, pain, fever, jaundice, rupture	Poor
HCC	10–12 years	M = F	Tender hepatomegaly, pain, anorexia, jaundice, fever, hemoperitoneum (rupture), increased alpha-fetoprotein level	Poor in extended cases; better if chemotherapy and surgery is applicable

plastic type. Epithelial HB is the most common type (60 %). It is subdivided into fetal and embryonal forms. Fetal epithelial HB is composed of cells smaller than normal hepatocytes, with a relatively low nucleus/cytoplasm ratio, eosinophilic cytoplasm, nucleoli, and few mitoses, growing either in a trabecular or compact pattern. Embryonal HB has a higher nucleus/cytoplasm ratio, basophilic cytoplasm, and ductal elements. The growth pattern is similar to that of the fetal type [5, 6].The mixed epithelial/mesenchymal type is less common than the epithelial type (30 % of cases). Mixed HB consists of an epithelial component (identical to epithelial HB), plus a mesenchymal component commonly including osteoid and chondroid elements with calcifications, hemorrhage, and necrosis (Fig. 1 d, e). Anaplastic HB accounts for only 10 % of cases. It is composed of monomorphous cells with scant cytoplasm and high mitotic rate. Infiltration of adjacent hepatocytes, vascular invasion, and necrosis is usually seen [4, 5, 6].

Regardless of the histologic type, all HBs are large with an average diameter at diagnosis of 10–12 cm. On cut sections, epithelial HB tends to be homogenous, whereas mixed HB has a more variegated appearance with large areas of calcification and hemorrhage. The right lobe is more frequently involved in the solitary form, whereas in multinodular HB both lobes may be involved. Anaplastic HB is frequently seen with massive central necrosis.

Although there are no definite pathogenetic factors in HB, associated congenital anomalies occur in up to 30 % of cases [5, 6]. Recently, a higher prevalence of HB has been described with familial polyposis and Gardner's syndrome [7].

The US appearance of HB varies according to the different histologic types. Usually, HBs are well delineated, multilobulated, and septated. Epithelial HB is frequently seen as a homogenous, hypoechoic mass, whereas mixed HB manifests as a heterogeneous mass with hyperechoic foci, due to calcifications, and hypo- or anechoic areas due to liquefactive necrosis [8, 9].

On non-enhanced CT, HB appears as a homogenous hypodense mass in the epithelial type and as a more heterogeneous mass in the mixed type. Calcifications can be detected in either type, small and delicate in epithelial HB and coarse and extensive in mixed HB [10, 11, 12, 13]. After contrast injection, enhancement of a thick peripheral rim (corresponding to viable tumor) or of septa may be seen in the early arterial phase (Fig. 1 a).

In MRI, epithelial HB presents as a homogenous mass, hypointense on T1-weighted and hyperintense on T2-weighted images. In the mixed type, depending on necrosis, hemorrhage, fibrosis, calcification, and the content of cartilage and septa, there may be a more heterogeneous aspect with hypointense bands on T1- and T2-weighted images and high-signal-intensity areas due to hemorrhage on both T1- and T2-weighted images (Fig. 1 b, c) [10, 14, 15].

Angiography reveals the hypervascular nature of the tumor, occasionally with a spoke-wheel pattern. Malignant neovascularization, stretching of vessels, pooling of contrast media, and invasion or encasement of branches of the portal vein or the hepatic artery and vein can be depicted. The latter findings are usually also seen by CT and MRI [3, 15, 16].

Infantile hemangioendothelioma

Infantile hemangioendothelioma (synonyms: angioendothelioma, cavernous angioma) is a primary benign, frequently symptomatic, vascular neoplasm that accounts for up to 12 % of all pediatric liver tumors.

Infantile hemangioendothelioma is the most common hepatic mass in the neonate. The majority (82 % of cases) of IHEs presents in the first 6 months of life, with only 5 % of the cases detected after the first year. Girls are more frequently affected than boys, with a ratio of approximately 1.4 to 2:1.

The most common form of presentation is that of an abdominal mass due to hepatomegaly. Additional clinical findings are: (a) congestive heart failure (25 % of cases) due to intratumoral high-flow arteriovenous shunts; (b) rarely, trapping of platelets by a massive IHE, resulting in thrombocytopenia (Kasabach-Meritt syndrome); (c) jaundice; and (d) rupture of a superficial IHE with hematoperitoneum [5, 16, 17]. Occasionally, IHE may be detected in utero, where the large arteriovenous shunts may lead to fetal hydrops. In these cases

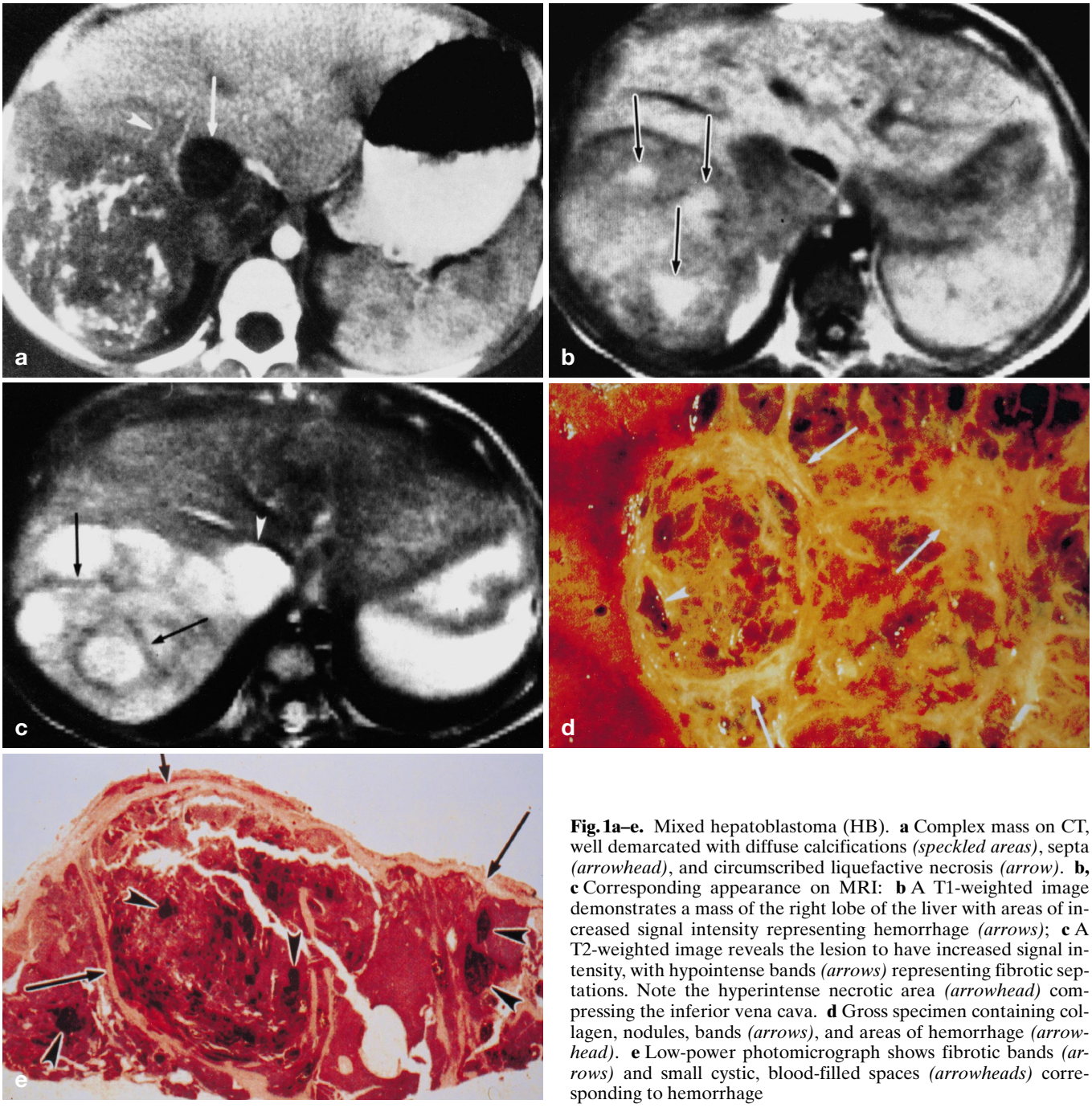

Fig. 1a–e. Mixed hepatoblastoma (HB). **a** Complex mass on CT, well demarcated with diffuse calcifications *(speckled areas)*, septa *(arrowhead)*, and circumscribed liquefactive necrosis *(arrow)*. **b, c** Corresponding appearance on MRI: **b** A T1-weighted image demonstrates a mass of the right lobe of the liver with areas of increased signal intensity representing hemorrhage *(arrows)*; **c** A T2-weighted image reveals the lesion to have increased signal intensity, with hypointense bands *(arrows)* representing fibrotic septations. Note the hyperintense necrotic area *(arrowhead)* compressing the inferior vena cava. **d** Gross specimen containing collagen, nodules, bands *(arrows)*, and areas of hemorrhage *(arrowhead)*. **e** Low-power photomicrograph shows fibrotic bands *(arrows)* and small cystic, blood-filled spaces *(arrowheads)* corresponding to hemorrhage

prenatal US can depict a liver mass together with polyhydramnios, cardiomegaly, anasarca, and ascites. In general, the prognosis is determined mainly by the amount of the shunt volume.

Histologically, two types are differentiated: type I with orderly proliferation of small vascular channels and cavernous areas; and type II with a more irregular structure, a higher mitotic rate, and a tendency of fibrosis (Fig. 2 f). Infantile hemangioendothelioma may be solitary, multiple, or diffuse, ranging in diameter from a few millimeters up to 15 cm with an average size between 0.5 and 3 cm (Fig. 2 e). In comparison with the multinodular and diffuse forms, solitary IHE has a much better prognosis. Symptomatic and asymptomatic tumors can undergo complete involution by 12–18 months after diagnosis. Often IHE is associated with other hemangiomas in skin, lung, trachea, spleen, thymus, lymph nodes, bone, and meninges [5, 18].

Plain-film radiography demonstrates a mass in the right upper quadrant of the abdomen, with speckled calcifications in approximately 16 %. In cases of massive intratumoral arteriovenous shunting, chest radiographs can show findings of congestive heart failure [19].

On scintigraphic studies with Tc-99-m tagged red blood cells there is increased uptake both in the early and delayed phases, in contrast to the findings in adult

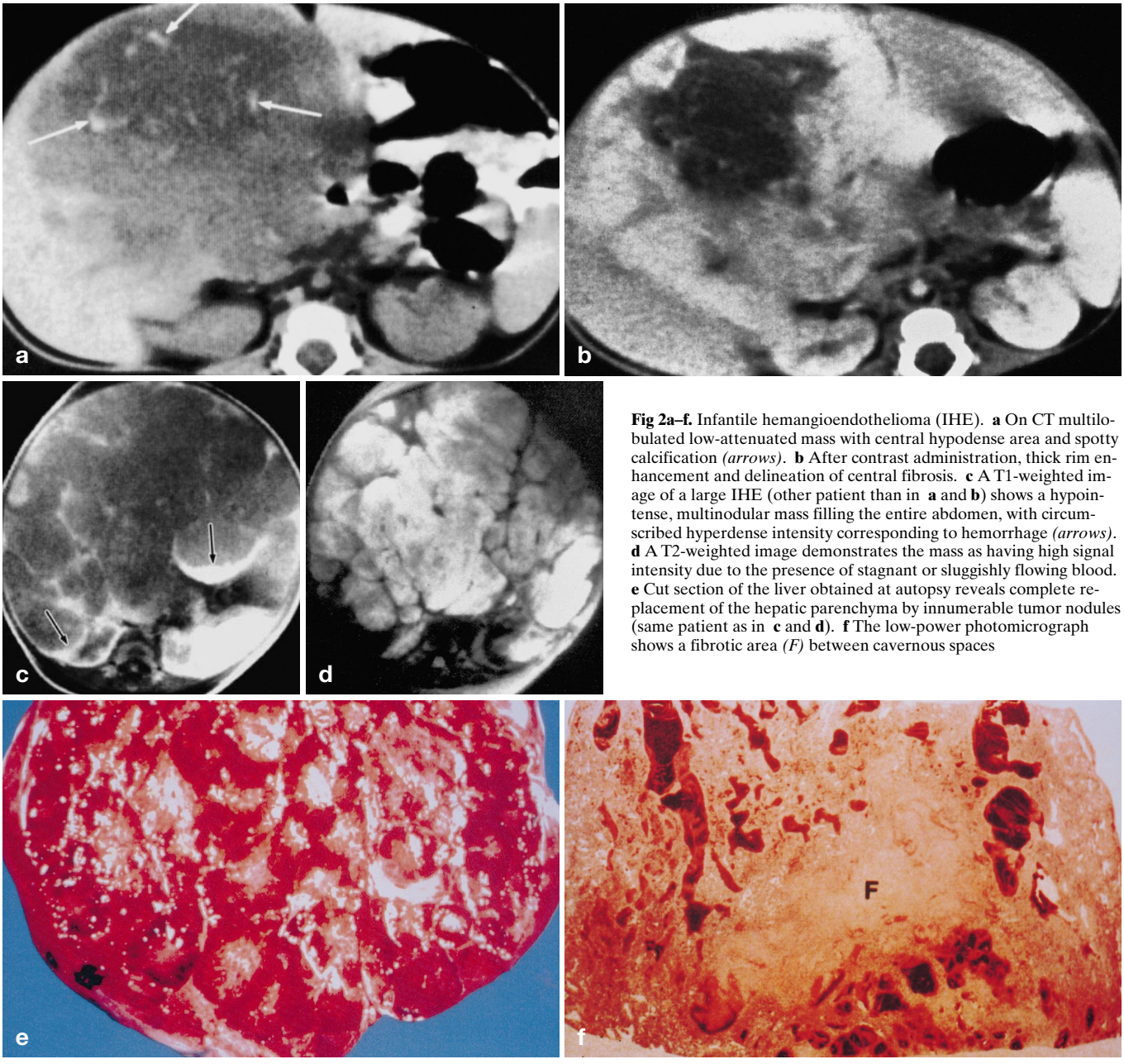

Fig 2a–f. Infantile hemangioendothelioma (IHE). **a** On CT multilobulated low-attenuated mass with central hypodense area and spotty calcification *(arrows)*. **b** After contrast administration, thick rim enhancement and delineation of central fibrosis. **c** A T1-weighted image of a large IHE (other patient than in **a** and **b**) shows a hypointense, multinodular mass filling the entire abdomen, with circumscribed hyperdense intensity corresponding to hemorrhage *(arrows)*. **d** A T2-weighted image demonstrates the mass as having high signal intensity due to the presence of stagnant or sluggishly flowing blood. **e** Cut section of the liver obtained at autopsy reveals complete replacement of the hepatic parenchyma by innumerable tumor nodules (same patient as in **c** and **d**). **f** The low-power photomicrograph shows a fibrotic area *(F)* between cavernous spaces

hemangioma where there is a early defect and a delayed uptake [18, 20, 21].

Infantile hemangioendothelioma in US usually shows well-defined margins and appears as a predominantly hypoechoic or complex mass or masses. In contrast to the appearance of adult hemangioma, only in a few cases IHE is hyperechoic. With involution IHE adopts a progressively increasing echogenic appearance. Doppler ultrasound can reveal venous flow in anechoic spaces of the lesion corresponding to intratumoral cavernous vascular channels. Increased flow within enlarged hepatic arteries and veins additionally supports the diagnosis of IHE [22].

In unenhanced CT, IHE presents as a single mass or multiple masses, with lower attenuation than the surrounding liver. After contrast administration, there is early peripheral enhancement with delayed progression to the center of the lesion; frequently, the central portion of large IHEs remains hypodense corresponding to central fibrosis (Fig. 2 a, b). Multifocal small lesions often show enhancement of the complete lesion [23, 24, 25, 26].

Depending on the degree of hemorrhage and necrosis, the MRI appearance of IHE varies. T1-weighted images show mostly a heterogeneous mass of low signal intensity, whereas on T2-weighted images a high signal intensity is seen. The high signal intensity on T2-weighted images is similar to that of hemangioma in adults. Occasionally, there is massive involvement of the liver by IHE with replacement of large portions of the normal parenchyma by the lesion. Thus, it can be difficult to identify the origin of tumor; however, the cavernous

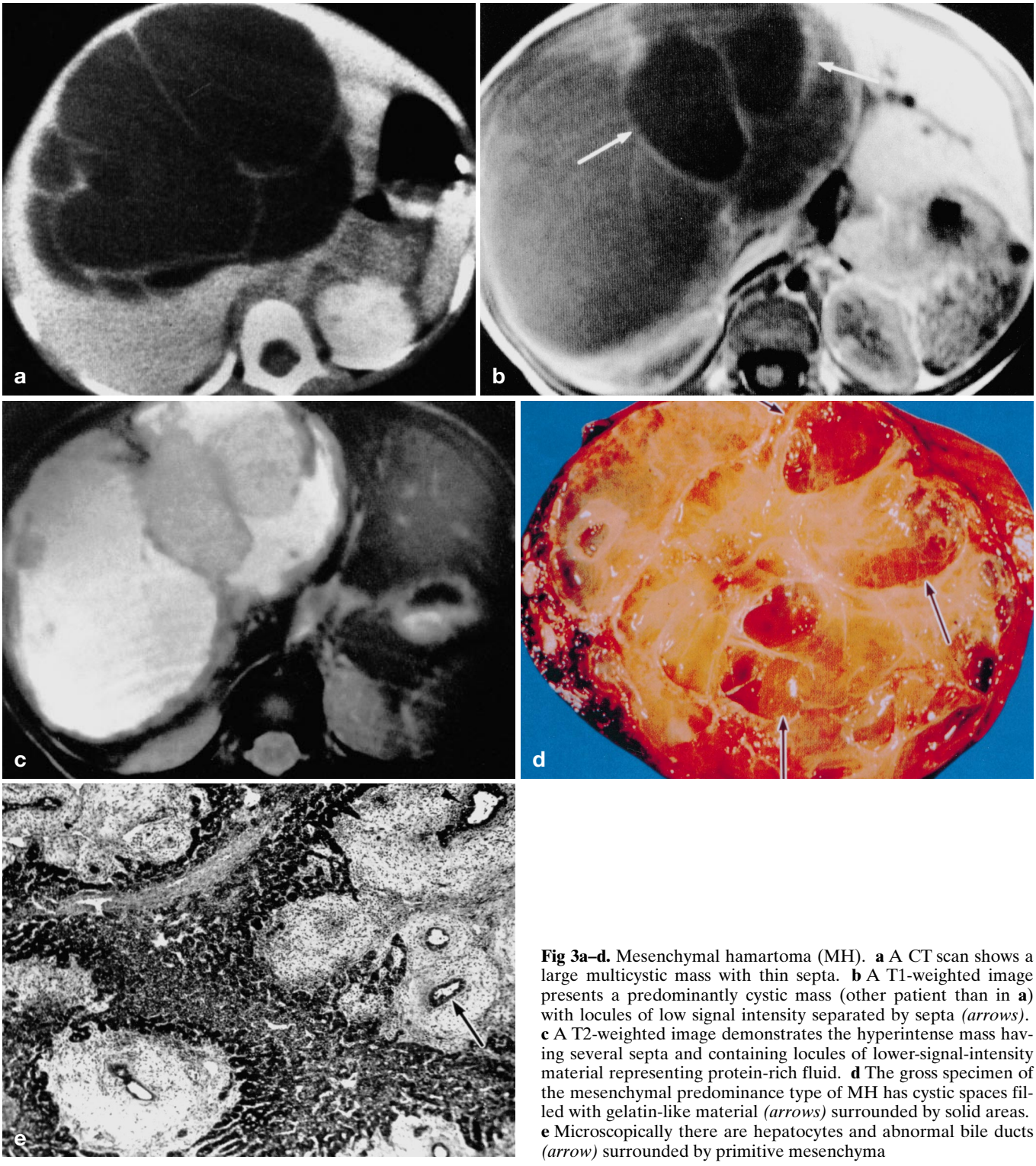

Fig 3a–d. Mesenchymal hamartoma (MH). **a** A CT scan shows a large multicystic mass with thin septa. **b** A T1-weighted image presents a predominantly cystic mass (other patient than in **a**) with locules of low signal intensity separated by septa *(arrows)*. **c** A T2-weighted image demonstrates the hyperintense mass having several septa and containing locules of lower-signal-intensity material representing protein-rich fluid. **d** The gross specimen of the mesenchymal predominance type of MH has cystic spaces filled with gelatin-like material *(arrows)* surrounded by solid areas. **e** Microscopically there are hepatocytes and abnormal bile ducts *(arrow)* surrounded by primitive mesenchyma

structure with the characteristic signal intensities on T1- and T2-weighted imaging may help in the diagnosis of a hemangiomatoid tumor (Fig. 2 c, d) [26, 27].

Angiography demonstrates decreased caliber of the aorta distal to the origin of the hepatic artery, an enlarged and tortuous hepatic artery, peripheral feeding vessels, intratumoral pooling of contrast media, and arteriovenous shunting with early draining veins [18, 28].

Mesenchymal hamartoma

Mesenchymal hamartoma (synonyms: bile duct fibroadenoma, lymphangioma, cavernous lymphangiomatoid tumor, giant lymphangioma, cystic mesenchymal hamartoma) is an uncommon tumor arising from the mesenchyma of the periportal tract. It accounts for 8 % of all hepatic tumors in childhood.

Mesenchymal hamartoma usually presents as a painless abdominal swelling without other symptoms. The age at presentation ranges from birth to 10 years with its peak between 15 and 20 months. It is slightly more frequent in boys than in girls [5, 14, 29, 30, 31].

The tumor is considered to be a developmental anomaly, rather than a true neoplasm, and consists of a mixture of bile ducts, hepatocytes, vessels, and mesenchyma without lymphatic vessels (Fig. 3e). Fluid accumulation in the mesenchymal tissue and cysts may be responsible for tumor growth.

Grossly, the tumor is mainly cystic, although occasionally a solid component is observed with small cystic areas, producing the so-called Swiss-cheese pattern (Fig. 3d). Therefore, two gross patterns are described: (a) cystic predominance; and (b) stromal predominance. The diameter of the mass ranges from 3 to 21 cm with an average of 18 cm [5, 29].

Plain abdominal radiographs and barium studies can reveal a right upper quadrant noncalcified mass that displaces the stomach, duodenum, transverse colon, and the right kidney [32].

Ultrasound reflects well the gross patterns, ranging from a predominantly anechoic mass with septa, corresponding to MH with cystic predominance, to a complex solid mass, corresponding to MH with stromal predominance [33, 34, 35].

Angiographically a large, hypo- to avascular mass is seen, with stretching of hepatic artery branches [36].

The appearance in CT also varies from a solid mass with small cystic, hypodense portions to a predominantly cystic mass with thin septa (Fig. 3a). After intravenous administration of contrast media, enhancement of the solid areas is detectable [10, 29, 30].

On T1- and T2-weighted MRI the cystic predominance type of MH may demonstrate varying signal intensities corresponding to different concentration of proteinaceous material within the locules (Fig. 3b, c). Due to fibrotic changes, the stromal predominance type demonstrates decreased signal intensity relative to the liver both on T1- and T2-weighted imaging [14, 29].

Undifferentiated embryonal sarcoma

Undifferentiated embryonal sarcoma (synonyms: undifferentiated sarcoma, embryonal sarcoma, malignant mesenchymoma, fibromyxosarcoma) is an uncommon malignant hepatic tumor (5% of pediatric liver tumors). In almost 90% of the cases, UES occurs in older children (8–12 years) and teenagers, without gender predilection.

Undifferentiated embryonal sarcoma presents as an abdominal mass with or without pain, fever, jaundice, and weight loss. Sometimes, the tumor may rupture followed by an acute abdominal crisis. There are no reliable changes in laboratory data, although mild leukocytosis and anemia in 50% of cases and elevated liver enzymes in 30% of cases are observed. Typically, serum alpha-fetoprotein levels are normal [5, 37].

Undifferentiated embryonal sarcoma is a large, mainly solid mass ranging in diameter from 7 to 20 cm. On macro-specimen, UES is frequently cystic due to large areas of necrosis and hemorrhage. The more solid portions of UES contain a gelatinous material. The tumor is mostly well delineated by a fibrotic pseudocapsule (Fig. 4c, d). Histologically the components of UES are undifferentiated spindle cells without any recognizable sarcomatous differentiation, resembling embryonal cells within a myxoid stroma [5, 37, 38].

Plain-film and barium studies delineate a right upper abdominal quadrant mass, with or without calcification, associated with displacement of adjacent structures and elevation of the right diaphragm.

The US appearance ranges from that of a multiseptated cystic mass, with cysts of variable size, to a heterogeneous solid mass (Fig. 4a). In solid UES, foci of calcification can cause high-level echoes with acoustical shadowing.

On CT, UES presents as a hypodense mass with attenuation values between water and muscle, traversed by dense septa. After intravenous contrast administration, both internal septa and peripheral rim (corresponding to a fibrous capsule) demonstrate enhancement (Fig. 4b). Undifferentiated embryonal sarcoma with internal attenuation in the range of water on CT scans corresponds grossly with myxoid-filled cystic tumors, whereas the more solid UESs are denser and may contain hemorrhagic and necrotic debris [39, 40].

On MRI, signal intensities of UES are heterogeneous but mostly hypointense on T1-weighted images, becoming hyperintense on T2-weighted images, correlating with the predominately cystic nature of the lesions. Hemorrhage, if present, results in high signal intensity on T1-weighted images, whereas the pseudocapsule and septations are of low signal on both T1- and T2-weighted images (Fig. 4e, f) [38, 41].

The angiographic appearance of UES is nonspecific. The lesion is usually hypovascular, and circumscribed areas of neovascularization are seen [38].

Hepatocellular carcinoma

Hepatocellular carcinoma accounts for up to 20% of primary pediatric liver tumors. Its histological and gross features are similar to the adult type, whereas the underlying etiologic conditions are largely different. Related disorders predisposing to HCC are biliary atresia, familial cholestasis, glycogen storage disease type I, hereditary tyrosinemia, hyperalimentation, and hepatitis B virus infection. However, in the majority of cases of HCC at the pediatric age, there are no pathogenetic factors. At the time of detection, age 10–12 years, children present with anorexia, abdominal pain, tender hepatomegaly, jaundice, hemoperitoneum (due to tumor rupture or erosion of surface vessels), and fever. Serum alpha-fetoprotein levels are markedly elevated (1000 ng/ml and higher) [2, 5, 15, 42].

The tumor cells resemble normal hepatocytes; therefore, differentiation from normal liver may be difficult

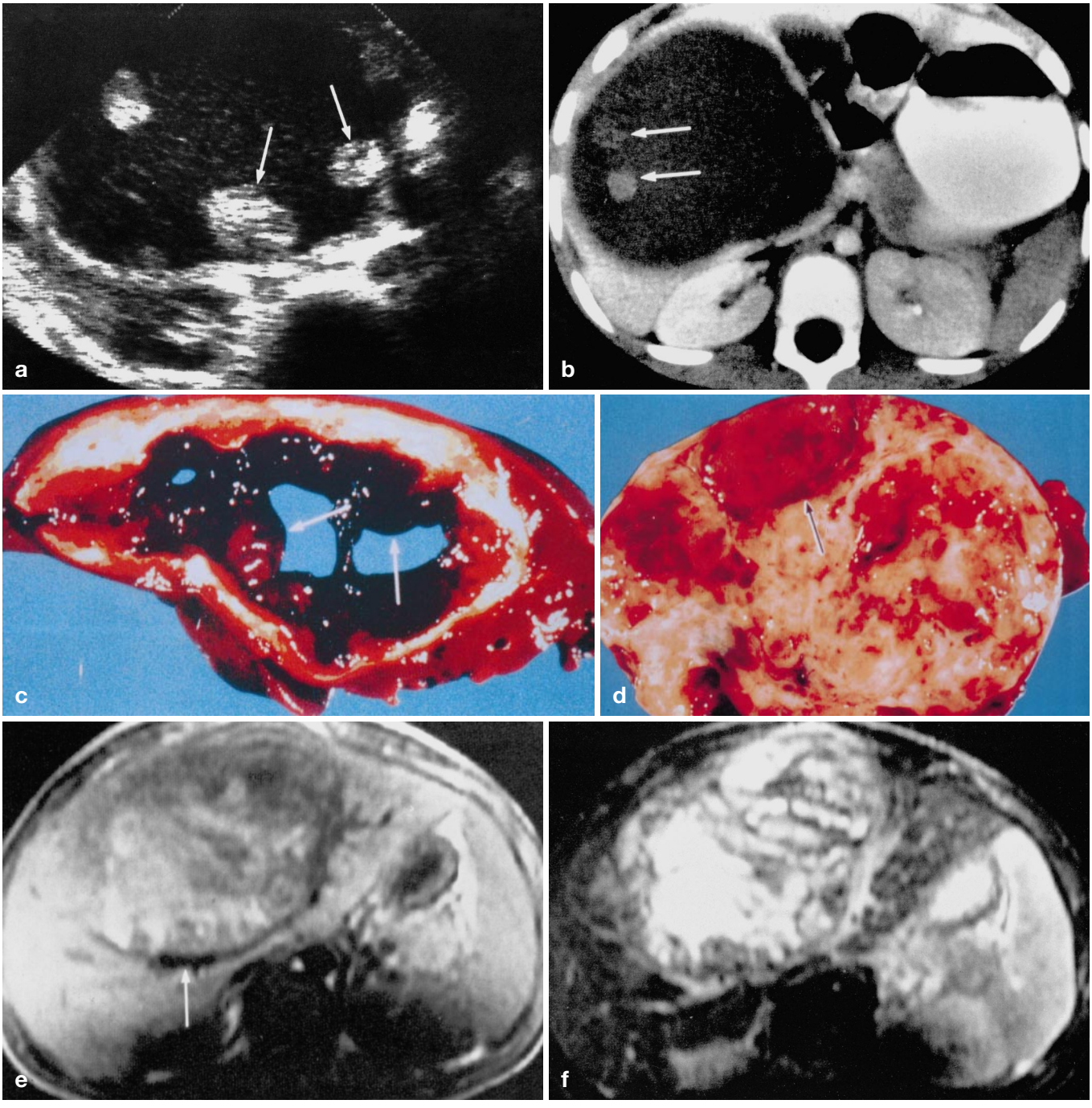

Fig. 4a–f. Undifferentiated embryonal sarcoma (UES). **a** Sonogram presents a cystic mass with large, echogenic, polypoid masses arising from its wall *(arrows)*. **b** A CT scan shows a predominantly cystic UES with a single septation and two slightly enhancing nodules *(arrows)*. **c** The correlating specimen confirms the cystic character of this UES, and shows in addition solid hemorrhagic masses *(arrows)* adhering to the wall of the tumor. **d** Gross specimen of a predominantly solid UES (other patient than in **a–c**) with circumscribed cystic, hemorrhagic changes *(arrows)*. **e** The T1-weighted image reveals a large hepatic mass of heterogeneous signal intensity (high-signal-intensity areas correspond to hemorrhage) compressing the right hepatic vein *(arrow)*. **f** On T2-weighted image the mass consists of regions with marked hyperintensity indicating hemorrhage

upon biopsy. The tumor grows in variable patterns: (a) solitary or massive (with or without capsule); (b) multifocal or nodular; and (c) diffuse, involving the entire liver. Necrosis sometimes results in a gross cystic appearance.

Due to the absence of Kupffer cells, sulfur colloid scintigraphy usually demonstrates solitary or multiple, space-occupying photopenic regions, whereas on gallium scans uptake is present [43].

On US, HCCs are predominantly hypoechoic and sometimes isoechoic with a thin hypoechoic halo corresponding to the tumor capsule. In diffuse HCC there is subtle disruption of the normal echo pattern, with anechoic areas due to necrosis [43, 44].

Table 2. Radiological findings in pediatric liver tumors

Tumor	US	CT	MRI	Angiography
HB	Well-delineated, septa, heterogeneous, hypoechoic (cysts, necrosis), calcification	Epithelial type: homogenous; mixed type: heterogeneous, peripheral rim enhancement, septa, calcification	Epithelial type: T1 hypointense, T2 hyperintense; mixed type: heterogeneous intensity on T1/T2	Malignant neovascularization, spoke-wheel pattern, vascular invasion
IHE	Well defined, predominantly hypoechoic, echogenic with involution, venous flow on Doppler US	Hypodense vs liver, peripheral enhancement, central fibrosis	T1: heterogeneous intensity; T2: hyperintense	Enlarged, tortuous hepatic artery, feeding vessels, pooling, arteriovenous shunts, early draining
MH	Cystic type: hypo- or anechoic, septa; solid type: heterogeneous	Cystic type: hypodense, septa; solid type: iso- or hyperdense, small cysts	Cystic type: T1, hetero- or hypointense; T2, hyperintense	Nonspecific hypo- or avascular, mass effect, stretching of vessels
UES	Cystic–multiseptated, heterogeneous, calcification	Hypodense, septa, calcification, peripheral rim enhancement, septa	T1: hypointense; T2: hyperintense, hemorrhage, peripheral rim, septa hypointense on T1/T2	Nonspecific, mostly hypovascular, mass effect
HCC	Hypoechoic, halo sign, diffuse: disorganization of normal pattern	Hypodense, calcification, hemorrhage, fatty metamorphosis, peripheral enhancement	T1: hypo- to hyperintense (due to necrosis, hemorrhage, septa, fat); T2: hyperintense	Malignant neovascularization, vascular invasion (e. g., tumor thrombus in veins)

Computed tomography reveals either a solitary, often well-defined mass with slightly lower attenuation than the normal liver or multiple, confluent masses, that occupy large areas of the liver. Occasionally, CT may detect diffuse tumor infiltration represented by a diffusely hypodense liver. Calcification, hemorrhage, necrosis, and fatty tumor metaplasia may be seen on unenhanced scans. Intravenous contrast administration improves the delineation of the lesion and may demonstrate a peripheral rim representing the tumor capsule [10, 42].

Although MRI may be superior to CT in characterizing HCC, its detection rate is similar for both imaging methods. In solitary HCC, T1-weighted images frequently demonstrate a mass with low signal intensity relative to normal liver; however, iso-, hyperintense, and mixed signal intensity patterns are also possible. On T2-weighted images a mass with moderately increased signal containing a mosaic pattern (due to necrosis, hemorrhage, septa, and fatty metaplasia) is a common finding. The intravenous administration of contrast (gadopentetate dimeglumine) may improve the detectability of small lesions, as well as multinodular and diffuse HCC on T1-weighted images, but normally there is no significant superiority to non-enhanced MRI.

Angiography displays the classic signs of malignant neovascularization: enlarged feeding arteries, tortuous vessels, early draining veins, pooling of contrast material, arteriovenous shunting, marked tumor blush, encasement of artery walls, and tumor thrombus in major veins [1, 10, 45].

In summary, the imaging features of juvenile HCC do not differ from those in adults.

Conclusion

Pediatric liver tumors are different from those that present in adults. The tumors discussed herein are unique to pediatric age, with the exception of HCC. To achieve a diagnosis it is essential to combine age/gender and clinical findings with radiologic appearance (Tables 1, 2). Imaging findings, particularly by US, CT, and MRI, provide in many cases sufficient information to achieve a specific diagnosis, obviating the need for biopsy.

The information derived from the analysis of imaging studies not only helps to diagnose a specific tumor, but also may guide the appropriate management of the patient.

References

1. Powers C, Ros PR, Stoupis C, Johnson WK, Segel KH (1994) Primary liver neoplasm: MR imaging with pathologic correlation. Radiographics 14: 459–482
2. Giacomantonio M, Ein SH, Mancer K, Stephens CA (1984) Thirty years of experience with pediatric primary malignant liver tumors. J Pediatr Surg 19: 523–526
3. Dachman AH, Pakter RL, Ros PR, Fishman EK, Goodman ZD, Lichtenstein JE (1987) Hepatoblastoma: radiologic–pathologic correlation in 50 cases. Radiology 164: 15–19
4. Lack EE, Neave C, Vawter GF (1982) Hepatoblastoma. A clinical and pathologic study of 54 cases. Am J Surg Pathol 6: 693–705
5. Craig JR (1994) Mesenchymal tumors of the liver. Diagnostic problems for the surgical pathologist. Pathology 3: 141–160
6. Craig JR, Peters RL, Edmondson HA (1989) Tumors of the liver and intrahepatic bile ducts. Atlas of tumor pathology, fascicle 26. Armed Forces Institute of Pathology, Washington, DC
7. Stoupis C, Ros PR (1993) Imaging findings in hepatoblastoma associated with Gardner's syndrome. AJR 161: 593–594
8. Bundscherer F, Deeg KH, Seiler A (1987) Sonographic diagnosis of solid space-occupying abdominal lesions in childhood. Monatsschr Kinderheilkd 135: 30–35
9. Men S, Hekimoglu B, Tuzun M, Arda IS, Pinar A (1995) Unusual US and CT findings in hepatoblastoma: a case report. Pediatr Radiol 25: 507–508
10. Boechat MI, Kangarloo H, Ortega J et al. (1988) Primary liver tumors in children: comparison of CT and MR imaging. Radiology 169: 727–732
11. Siegel MJ, Herman TE (1992) Periportal low attenuation at CT in childhood. Radiology 183: 685–688
12. King SJ, Babyn PS, Greenberg ML, Phillips MJ, Filler RM (1993) Value of CT in determining the resectability of hepatoblastoma before and after chemotherapy. AJR 160: 793–798

13. Plumley DA, Grosfeld JL, Kopecky KK, Buckwalter KA, Vaughan WG (1995) The role of spiral (helical) computerized tomography with three-dimensional reconstruction in pediatric solid tumors. J Pediatr Surg 30: 317–321
14. Balmer B, LeCoultre C, Feldges A, Hanimann B (1996) Mesenchymal liver hamartoma in a newborn: case report. Eur J Pediatr Surg 6: 303–305
15. Okada A, Fukuzawa M, Oue T et al. (1998) Thirty-eight years experience of malignant hepatic tumors in infants and childhood. Eur J Pediatr Surg 8: 17–22
16. Schweinitz D von, Gluer S, Mildenberger H (1995) Liver tumors in neonates and very young infants: diagnostic pitfalls and therapeutic problems. Eur J Pediatr Surg 5: 72–76
17. Dachman AH, Lichtenstein JE, Friedman AC, Hartman DS (1983) Infantile hemangioendothelioma of the liver: a radiologic–pathologic–clinical correlation. AJR 140: 1091–1096
18. Keslar PJ, Buck JL, Selby DM (1993) From the archives of the AFIP. Infantile hemangioendothelioma of the liver revisited. Radiographics 13: 657–670
19. Leary DL, Weiskittel DA, Blane CE, Coran AG (1989) Follow-up imaging of benign pediatric liver tumors. Pediatr Radiol 19: 234–236
20. Miller JH (1987) Technetium-99m-labeled red blood cells in the evaluation of hemangiomas of the liver in infants and children. J Nucl Med 28: 1412–1418
21. Gianni W, Vincentis G de, Graziano P et al. (1997) Scintigraphic imaging of hepatic epithelioid hemangioendothelioma. Digestion 58: 498–500
22. Miller JH, Greenspan BS (1985) Integrated imaging of hepatic tumors in childhood. Part II. Benign lesions (congenital, reparative, and inflammatory). Radiology 154: 91–100
23. Lucaya J, Enriquez G, Amat L, Gonzalez-Rivero MA (1985) Computed tomography of infantile hepatic hemangioendothelioma. AJR 144: 821–826
24. Shin MS, Carpenter JT Jr, Ho KJ (1991) Epithelioid hemangioendothelioma: CT manifestations and possible linkage to vinyl chloride exposure. J Comput Assist Tomogr 15: 505–507
25. Yoshikawa J, Matsui O, Kadoya M, Gabata T, Arai K, Takashima T (1992) Delayed enhancement of fibrotic areas in hepatic masses: CT-pathologic correlation. J Comput Assist Tomogr 16: 206–211
26. Van Beers B, Roche A, Mathieu D et al. (1992) Epithelioid hemangioendothelioma of the liver: MR and CT findings. J Comput Assist Tomogr 16: 420–424
27. Berger TM, Berger MF, Hoffman AD, Zimmerman D, Tonz O (1994) Imaging diagnosis and follow-up of infantile hepatic haemangioendothelioma: a case report. Eur J Pediatr 153: 100–102
28. Burke DR, Verstandig A, Edwards O, Meranze SG, McLean GK, Stein EJ (1986) Infantile hemangioendothelioma: angiographic features and factors determining efficacy of hepatic artery embolization. Cardiovasc Intervent Radiol 9: 154–157
29. Ros PR, Goodman ZD, Ishak KG et al. (1986) Mesenchymal hamartoma of the liver: radiologic–pathologic correlation. Radiology 158: 619–624
30. Maioribus CA de, Lally KP, Sim K, Isaacs H, Mahour GH (1990) Mesenchymal hamartoma of the liver. A 35-year review. Arch Surg 125: 598–600
31. Alwaidh MH, Woodhall CR, Carty HT (1997) Mesenchymal hamartoma of the liver: a case report. Pediatr Radiol 27: 247–249
32. Wholey MH, Wojno KJ (1994) Pediatric hepatic mesenchymal hamartoma demonstrated on plain film, ultrasound and MRI, and correlated with pathology. Pediatr Radiol 24: 143–144
33. Hirata GI, Matsunaga ML, Medearis AL, Dixon P, Platt LD (1990) Ultrasonographic diagnosis of a fetal abdominal mass: a case of a mesenchymal liver hamartoma and a review of the literature. Prenat Diagn 10: 507–512
34. Megremis S, Sfakianaki E, Voludaki A, Chroniaris N (1994) The ultrasonographic appearance of a cystic mesenchymal hamartoma of the liver observed in a middle-aged woman. J Clin Ultrasound 22: 338–341
35. Bejvan SM, Winter TC, Shields LE et al. (1997) Prenatal evaluation of mesenchymal hamartoma of the liver: gray scale and power Doppler sonographic imaging. J Ultrasound Med 16: 227–229
36. Yandza T, Valayer J (1986) Benign tumors of the liver in children: analysis of a series of 20 cases. J Pediatr Surg 21: 419–423
37. Walker NI, Horn MJ, Strong RW et al. (1992) Undifferentiated (embryonal) sarcoma of the liver. Pathologic findings and long-term survival after complete surgical resection. Cancer 69: 52–59
38. Ros PR, Olmsted WW, Dachman AH, Goodman ZD, Ishak KG, Hartman DS (1986) Undifferentiated (embryonal) sarcoma of the liver: radiologic–pathologic correlation. Radiology 161: 141–145
39. Moon WK, Kim WS, Kim IO et al. (1994) Undifferentiated embryonal sarcoma of the liver: US and CT findings. Pediatr Radiol 24: 500–503
40. Moon WK, Kim WS, Choi BI, Kim IO, Yeon KM, Han MC (1995) Undifferentiated embryonal sarcoma of the liver treated with chemotherapy: CT imaging in four patients. Abdom Imaging 20: 133–137
41. Yoon W, Kim JK, Kang HK (1997) Hepatic undifferentiated embryonal sarcoma: MR findings. J Comput Assist Tomogr 21: 100–102
42. Gururangan S, A OM, MacMahon C et al. (1992) Primary hepatic tumours in children: a 26-year review. J Surg Oncol 50: 30–36
43. Miller JH, Greenspan BS (1985) Integrated imaging of hepatic tumors in childhood. Part I. Malignant lesions (primary and metastatic). Radiology 154: 83–90
44. Mathieu D, Guinet C, Bouklia-Hassane A, Vasile N (1988) Hepatic vein involvement in hepatocellular carcinoma. Gastrointest Radiol 13: 55–60
45. Buetow PC, Midkiff RB (1997) MR imaging of the liver. Primary malignant neoplasms in the adult. Magn Reson Imaging Clin North Am 5: 289–318